TURBULENCE IN EXTRASOLAR PLANETARY SYSTEMS IMPLIES THAT MEAN MOTION RESONANCES ARE RARE

Fred C. Adams[1,2], Gregory Laughlin[3], and Anthony M. Bloch[1,4]

[1]*Michigan Center for Theoretical Physics*
Physics Department, University of Michigan, Ann Arbor, MI 48109

[2]*Astronomy Department, University of Michigan, Ann Arbor, MI 48109*

[3]*Lick Observatory, University of California, Santa Cruz, CA 95064*

[4]*Department of Mathematics, University of Michigan, Ann Arbor, MI 48109*

ABSTRACT

This paper considers the effects of turbulence on mean motion resonances in extrasolar planetary systems and predicts that systems rarely survive in a resonant configuration. A growing number of systems are reported to be in resonance, which is thought to arise from the planet migration process. If planets are brought together and moved inward through torques produced by circumstellar disks, then disk turbulence can act to prevent planets from staying in a resonant configuration. This paper studies this process through numerical simulations and via analytic model equations, where both approaches include stochastic forcing terms due to turbulence. We explore how the amplitude and forcing time intervals of the turbulence affect the maintenance of mean motion resonances. If turbulence is common in circumstellar disks during the epoch of planet migration, with the amplitudes indicated by current MHD simulations, then planetary systems that remain deep in mean motion resonance are predicted to be rare. Specifically, the fraction of resonant systems that survive over a typical disk lifetime of ~ 1 Myr is less than ~ 0.025. If mean motion resonances are found to be common, their existence would place tight constraints on the amplitude and duty cycle of turbulent fluctuations in circumstellar disks. These results can be combined by expressing an upper limit on the fraction of surviving resonant systems in the form $\mathcal{P}_{\mathrm{bound}} \approx C/N_{\mathrm{orb}}^{1/2}$, where C is a dimensionless parameter of order unity and N_{orb} is the number of orbits for which turbulence is active.

Subject headings: MHD — planetary systems — planetary systems: formation — planets and satellites: formation — turbulence

1. INTRODUCTION

An increasing number of the observed extrasolar planetary systems have been discovered to contain multiple planets. A growing subset of these multiple planet systems have period ratios close to the ratios of small integers and hence are candidates for being in mean motion resonance (e.g., Mayor et al. 2001, Marcy et al. 2002, Butler et al. 2006). In true resonant configurations, the orbital frequencies not only display integer ratios, but, in addition, the relevant resonant arguments (angular variables composed of the osculating orbital elements) display constrained oscillatory time evolution (for further discussion, see Murray & Dermott 1999; hereafter MD99; see also Peale 1976). As a result, these resonant configurations represent rather special dynamical states of the planetary system and their existence (if/when observed) places interesting constraints on the formation and long term evolution of these systems. More specifically, as we show in this paper, planetary systems are easily knocked out of mean motion resonance. One source of perturbations acting on the planets is turbulent fluctuations in the circumstellar disks that originally formed the planets. Since these disks are also necessary ingredients in the current picture of planetary migration (e.g., Papaloizou & Terquem 2006), and since coupled migration seems necessary to put planets into mean motion resonance (e.g., Lee & Peale 2002; Lee 2004; Moorhead & Adams 2005; Beaugé et al. 2006), the effects of disk turbulence on the resonances is important to understand.

This paper analyzes the effects of turbulence on planets in or near mean motion resonance using both a semi-analytic treatment (§2) and direct numerical integrations (§3). The semi-analytic approach makes extreme approximations in order to obtain tractable equations, but it allows for an explicit determination of how the long term behavior depends on the basic physical variables (e.g., planet masses, semimajor axes, type of resonance, turbulent forcing amplitude, etc.). In contrast, numerical integrations can be carried out to high accuracy includng all 18 dynamical variables of the problem (for 3-body systems). Although the simulations demonstrate what the long term behavior will be, they don't automatically specify the relationships between the aforementioned physical variables. Fortunately, both approaches give consistent results for the intermediate time scales of interest. In particular, we find that the expectation value of the effective energy of the resonance – considered as a nonlinear oscillator – increases linearly with time. Similarly, the probability that systems stay in resonance decreases with time. For the stochastic pendulum model, the fraction of systems in resonance decreases as the square root of time for the simplest case in which the systems freely random walk in and out of a bound state; the decay is exponential if systems cannot return to resonance after leaving. The full numerical integrations give results that are intermediate between these extremes. For the model equations, the leading coefficients in the time-dependent relationships are given by the amplitude of the fluctuations, the time intervals of their forcing, and the natural oscillation frequency of the libration angle of the

original resonance. This paper thus provides a relatively simple description of the effects of turbulent fluctuations on planetary systems in or near mean motion resonance.

2. SEMI-ANALYTIC MODEL EQUATIONS

2.1. Pendulum Model for the Resonance

For the sake of definiteness, we consider the case in which a larger planet on an external orbit perturbs a smaller planet on an interior orbit. The larger body is then assumed to have orbital elements that do not change with time (or at least vary much less than those of the smaller inner planet). We are thus making the most extreme approximation and keeping only the leading order terms in order to obtain an analytic description. Following MD99, the equation of motion for the libration angle φ for two planets in resonance reduces to that of a pendulum, i.e.,

$$\frac{d^2\varphi}{dt^2} + \omega_0^2 \sin \varphi = 0 \,, \tag{1}$$

where the natural oscillation frequency ω_0 is given by

$$\omega_0^2 = -3j_2^2 \mathcal{C}_r \Omega e^{|j_4|} \,. \tag{2}$$

Here, Ω and e are the mean motion and eccentricity of the inner planet. The integers j_2 and j_4 depend on the type of resonance being considered. The parameter $\mathcal{C}_r$, which is taken to be constant, is given by

$$\mathcal{C}_r = \mu \Omega \, \alpha f_d(\alpha) \,, \tag{3}$$

where $\mu = m_{\text{out}}/M_*$ and where m_{out} is the mass of the outer (perturbing) planet. The quantity $\alpha f_d(\alpha)$ results from the expansion of the disturbing function (MD99), where the parameter α is the ratio of the semimajor axes of the two planets, i.e., $\alpha \equiv a_1/a_2$. This approximation neglects terms of order $\mathcal{O}(\mu)$. Finally, we note that more complicated analytic models for mean motion resonances can be derived (e.g., Holman & Murray 1996; Quillen 2006), but they are qualitatively similar to the pendulum equation considered here.

For much of this analysis, we are interested in the 2:1 mean motion resonance since observed extrasolar planetary systems are (sometimes) found in or near such a configuration, and since these resonances are generally the strongest. For this case, the integers $j_2 = -1$ and $j_4 = -1$. For the 2:1 resonance, $\alpha f_d(\alpha) \approx -3/4$, where α is the ratio of semimajor axes of the two planets. With these specifications, the natural oscillation frequency ω_0 of the libration angle is given approximately by

$$\omega_0^2 \approx \frac{9}{4}\mu\Omega^2 \, e \,. \tag{4}$$

In typical cases, where planet masses are 1000 times smaller than the stellar masses, and the eccentricity $e \sim 0.1$, we find that $\omega_0/\Omega \sim 10^{-2}$. As a result, the period of oscillation for the libration angle is typically ~ 100 orbits.

For completeness, we note that for first order resonances, the oscillation frequency ω_0^2 often has additional contributing terms (MD99). The order of the additional terms differs from that of equation (2) by a factor of order $\mathcal{O}(\mu/e^3)$, where e is the eccentricity of the inner planet. Under some circumstances of interest, $\mu \sim 10^{-3}$ and $e \sim 0.1$, so this correction can be of order unity. We are thus considering only the simplest form of the pendulum equation in this analysis. In principle, however, care must be taken to include all of the relevant terms.

2.2. Turbulent Perturbations

Given the pendulum model for the resonance (from MD99), the next step is to include the effects of additional perturbations produced by turbulence in the circumstellar disk material that remains after the planets have been formed. Since this disk material is generally thought to induce planetary migration, some disk material is likely to be present, for a typical time scale of $1 - 10$ Myr. Under many circumstances, these disks are expected to be turbulent (Balbus & Hawley 1991) due to the magneto-rotational instability (MRI). Although MRI can be shut down if the ionization rate is not high enough, star forming regions can experience enhanced cosmic ray fluxes, and hence enhanced ionization rates, due to cosmic rays from supernovae becoming trapped in the magnetic fields of molecular clouds (Fatuzzo et al. 2006). In any case, we consider turbulent fluctuations to be present and consider our previous model (Laughlin et al. 2004; hereafter LSA) to provide the parameters of the perturbations.

In principle, the turbulent fluctuations in the disk can affect either planet, i.e., the outer perturbing planet (in this analysis) or the inner perturbed planet. If the outer planet is subject to turbulent fluctuations, they have the affect of shaking the effective base of the pendulum. As a result, they modify the effective potential energy of the pendulum, and the stochastic term enters into the equation of motion as follows:

$$\frac{d^2\varphi}{dt^2} + [\omega_0^2 + \xi(t)] \sin \varphi = 0 \,, \tag{5}$$

where $\xi(t)$ is the stochastic forcing term. This is the form expected when the circumstellar disk surrounds both planets and primarily influences the outer one. In contrast, if the disk (the torques produced by turbulence in the disk) primarily influences the inner planet, then the fluctuations provide an additional acceleration term and the equation of motion takes

the form

$$\frac{d^2\varphi}{dt^2} + \omega_0^2 \sin\varphi = -\widetilde{\xi}(t) \,. \tag{6}$$

For the sake of simplicity, we will primarily consider the first case (eq. [5]). Notice also that both types of fluctuations can be included.

The inclusion of turbulent fluctuations thus provides a stochastic forming term in the pendulum equation of motion (1). The forcing term $\xi(t)$ can be considered as a series of "kicks" produced by short-term forcing due to turbulence. To completely specify this forcing effect, one needs to determine the spectrum of fluctuation amplitudes, the timing of the fluctuations, and any possible correlations in the fluctuation timing. This latter property determines the so-called "color" of the noise (fluctuations) and can have (perhaps) surprising effects on the long-term evolution of the stochastic pendulum and hence the resonance angles of the planetary system (Mallick & Marcq 2004, hereafter MM04).

The formulation for turbulence developed in LSA shows that the turbulent fluctuations are reloaded into the disk on roughly an orbital time scale. In order to consider the turbulent torques to be fully independent, we must use the longest relevant orbital period, which corresponds to that of the outer disk edge (in the calculations of LSA). This period at the outer disk edge is about twice that of the planet being forced. Since the outer (perturbing) planet is being forced by the turbulence in the present context, and since the outer planet is in a 2:1 mean motion resonance with the inner planet, this turbulent forcing period is approximately four times the period of the inner planet.

Next we need to account for the fluctuations in the equation of motion. To the same order of approximation used to derive the pendulum equation for the resonance, the time rate of change of the mean motion is given approximately by

$$\frac{d\Omega}{dt} \approx -\frac{1}{3}\Omega\left(\frac{1}{J}\frac{dJ}{dt}\right) \,, \tag{7}$$

where J is the angular momentum of the inner planetary orbit. Here we consider the turbulent fluctuations to provide discrete changes in the angular momentum on time scales comparable to the orbital period P_D at the disk edge, where (as discussed above) we expect $P_D \approx 4P_{orb} = 4(2\pi/\Omega)$. Thus, the time scale Δt for independent stochastic perturbations to act is given by $\Delta t \approx 8\pi/\Omega$. Since $d^2\varphi/dt^2 \sim d\Omega/dt$ (from the derivation of MD99), the amplitude of the stochastic forcing term can be written

$$\xi_k \approx -\frac{\Omega^2}{24\pi}\left(\frac{\Delta J}{J}\right)_k \,, \tag{8}$$

where the subscript 'k' indicates that this increment of force (or angular momentum) is delivered at discrete time intervals, which can be counted and hence labeled with an integer

k. The last factor represents the fractional change in the angular momentum of the planet per realization of the turbulence, i.e., per time interval Δt.

The amplitude $[(\Delta J)/J]_k$ is calculated in LSA. For turbulent fluctuations at the "critical amplitude", that required for turbulent torques to dominate over Type I migration torques, $[(\Delta J)/J]_k \sim 5 \times 10^{-5}$. For larger fluctuations that allow turbulent torques to dominate long enough to save migrating planetary cores, they find that $[(\Delta J)/J]_k \sim 2 \times 10^{-2}$. Three dimensional MHD simulations generally produce fluctuations with amplitudes between these two benchmark values, with some preference for the larger portion of the range (e.g., Nelson 2005).

Since the forcing amplitude $[(\Delta J)/J]_k$ plays an important role, it is useful to have an heuristic understanding of the expected value. For a circumstellar disk with surface density Σ, the torque exerted on a planet can be written in terms of the benchmark value $T_D = 2\pi G \Sigma r m_{\rm p}$. The torque due to turbulence is expected to be a fraction f_T of this physical scale, where numerical simulations suggest that $f_T \approx 0.05$ (e.g., Johnson et al. 2006; Nelson 2005). This torque acts over a time interval to produce a change in angular momentum. As argued above, this calculation uses a time interval of four orbital periods, long enough so that the turbulent torques can be taken to be independent. The torque thus acts on a timescale $4P_{orb} = 8\pi (r^3/GM_*)^{1/2}$ and the net change in angular momentum $(\Delta J) = 4P_{orb} f_T T_D$. Finally, the orbital angular momentum J of the planet is given by $J = m_{\rm p}[GM_* r(1 - e^2)]^{1/2}$. We can absorb the eccentricity dependence into the definition of f_T. Putting these results together, we can write the fractional change in angular momentum over one time interval $(4P_{orb})$ in the form

$$\left(\frac{\Delta J}{J}\right)_k = f_T \frac{16\pi^2 \Sigma r^2}{M_*} \approx 10^{-3} \left(\frac{\Sigma}{1000 {\rm g\, cm}^{-2}}\right), \tag{9}$$

where the second equality is scaled for a 1 AU orbit and a typical surface density at that radius. Note that we expect the surface density profile to have a nearly power-law form $\Sigma \sim r^{-p}$, where $p \sim 3/2$, so the quantity Σr^2 varies slowly with radius.

2.3. Time Evolution of the Stochastic Pendulum

With the mean motion resonance modeled by a pendulum equation, and with the characteristics of the turbulent fluctuations specified, we now find the time evolution of the system. If we define a dimensionless time variable

$$\tau \equiv \omega_0 t, \tag{10}$$

where ω_0 is the natural oscillation frequency of the libration angle, and is defined by equation (4), then the equation of motion reduces to the form

$$\frac{d^2\varphi}{d\tau^2} + [1 + \eta(\tau)]\sin\varphi = 0\,, \tag{11}$$

where the stochastic forcing term can be written in the form

$$\eta(\tau) = \eta_k \delta\left([\tau] - \Delta\tau\right)\,, \tag{12}$$

where $\delta(x)$ is the Dirac delta function. In this formulation, $\Delta\tau$ is the time interval between stochastic kicks, the dimensionless time variable is measured mod-$\Delta\tau$, and the amplitude of the kicks is given by

$$\eta_k = \frac{\xi}{\omega_0^2} = -\frac{1}{24\pi}\left(\frac{\Omega}{\omega_0}\right)^2\left(\frac{\Delta J}{J}\right)_k\,. \tag{13}$$

The quantity η_k is thus a stochastic variable that has a distribution of values inherited from the distribution of values of $[(\Delta J)/J]_k$, which in turn is determined by the properties of the turbulence. The kicks in angular momentum can be either positive or negative, with no expected asymmetry, so that $\langle\eta_k\rangle = 0$. We can characterize the amplitude by the RMS (root-mean-square) of the variable. Using the amplitudes expected from numerical MHD simulations (see LSA and the previous subsection), this amplitude is expected to lie in the range

$$\eta_{\rm rms} = \langle\eta_k^2\rangle^{1/2} \approx 0.007 - 2.4\,, \tag{14}$$

with a typical value of $\eta_{\rm rms} \approx 0.13$ (from the benchmark value of eq. [9]). These acceleration kicks occur at typical time intervals $\Delta t \approx 8\pi/\Omega$, which sets the corresponding dimensionless time interval to be $\Delta\tau \approx 8\pi\omega_0/\Omega$. In general, both the amplitudes and the time intervals between forcing will vary from cycle to cycle according to their (respective) distributions. However, we can scale out the time variations (see Appendix A and Adams & Bloch 2008), and, furthermore, our characterization of the turbulence is formulated with a well-defined (single-valued) forcing time. As a result, we present the remainder of this analysis using a single forcing time interval and focus on the effects of the distribution of forcing amplitudes η_k.

To analyze the behavior of the stochastic pendulum, as defined above, it is useful to work in terms of phase space variables. We thus rewrite the equation of motion into two parts, i.e.,

$$\frac{d\varphi}{d\tau} = V\,, \qquad \text{and} \qquad \frac{dV}{d\tau} = -\left[1 + \eta\right]\sin\varphi\,. \tag{15}$$

We then define the probability distribution function for the phase space variables, $P(\varphi, V; t)$, which obeys the Fokker-Planck equation (MM04; Binney & Tremaine 1987)

$$\frac{\partial P}{\partial\tau} + V\frac{\partial P}{\partial\varphi} - \sin\varphi\frac{\partial P}{\partial V} = \frac{\mathcal{D}}{2}\sin^2\varphi\frac{\partial^2 P}{\partial V^2}\,, \tag{16}$$
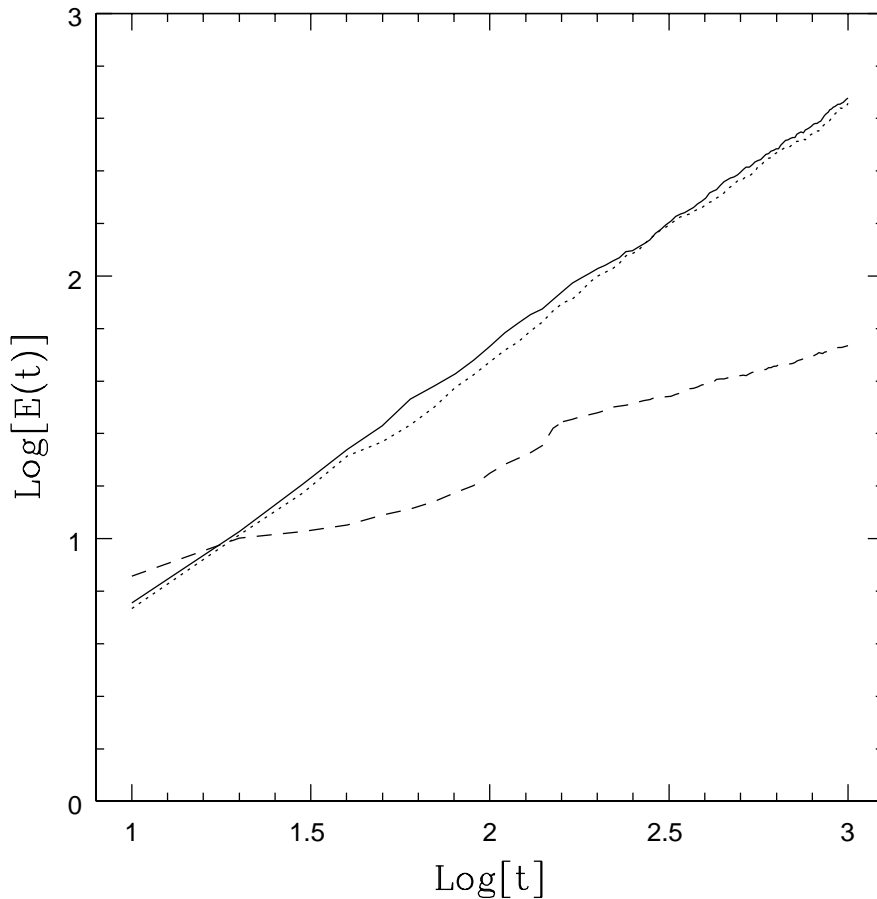
Fig. 1.— Mean time evolution of the energy of a stochastic pendulum with noise terms of various "colors". For each curve/line, 1000 realizations of the time evolution of the oscillator have been averaged together. The curves show the results for white noise (solid), pink noise (dotted), and brown noise (dashed). The first two types of noise lead to energy evolution that is linear in time, $\langle E \rangle \sim t$, whereas brown noise leads to energy that increases $\langle E \rangle \sim \sqrt{t}$.

where the phase space diffusion constant $\mathcal{D}$ is set by the amplitude of the fluctuation spectrum. Specifically, we can write the diffusion constant in terms of previously defined variables,

$$\mathcal{D} = \frac{\langle \eta_k^2 \rangle}{\Delta \tau} \approx \frac{\langle \eta_k^2 \rangle \Omega}{8\pi \omega_0} \, . \tag{17}$$

Next we argue that the libration angle φ varies rapidly compared to the velocity V. This claim can be verified by noting that $dV/d\tau \sim \eta_k$ so that $V \sim \tau^{1/2}$ (since the random variable η_k implies a random walk growth). However, the libration angle obeys the equation $d\varphi/d\tau = V$, which in turn implies that $\varphi \sim \tau^{3/2}$ (see MM04 for further discussion). In the long term, the libration angle thus varies faster than V and we can average the Fokker-Planck equation over the angle φ to obtain the time evolution equation for the averaged probability distribution function $p(V; \tau)$, i.e.,

$$\frac{\partial p}{\partial \tau} = \langle \sin^2 \varphi \rangle \frac{\mathcal{D}}{2} \frac{\partial^2 p}{\partial V^2} \, . \tag{18}$$

This equation has the well-known solution

$$p(V; \tau) = \frac{1}{(\pi D \tau)^{1/2}} \exp \left[-\frac{V^2}{D\tau} \right] \, , \tag{19}$$

where we have defined an effective diffusion constant $D = 2\mathcal{D}\langle \sin^2 \varphi \rangle$. In the long time limit, $\varphi \sim \tau^{3/2}$, and the angle fully samples the range $[0, 2\pi]$, so that $\langle \sin^2 \varphi \rangle = 1/2$ and hence $\mathcal{D} = D$. Notice also that the velocity V grows as $V \sim \tau^{1/2}$ in the long time limit. Since the energy of the pendulum grows large at long times, the kinetic term dominates the potential energy term, and the energy $E \approx V^2/2$. With this substitution, the probability distribution function for the energy takes the simple form

$$P(E; \tau) = \left(\frac{2}{\pi D \tau} \right)^{1/2} E^{-1/2} \exp \left[-\frac{2E}{D\tau} \right] \, . \tag{20}$$

This result implies that the expectation value of the energy grows linearly with time in the long time limit, i.e.,

$$\langle E \rangle = \frac{D}{4} \tau \, . \tag{21}$$

This linear time dependence can be understood in terms of a random walk of velocity, as shown in Appendix B.

This time behavior is seen in numerical simulations of the stochastic pendulum equation. Figure 1 shows the time development of the mean energy, averaged over 10^4 realizations, for three different types of fluctuations. The solid curve shows white noise, where the fluctuation amplitude and the time interval Δt between kicks are uniformly distributed about

well-defined mean values. The dotted curve shows the case of "pink" noise, in which the distribution of time intervals is taken to have a decaying exponential form; this distribution leads to more time intervals near the lower end of the spectrum. As long as the mean time interval and mean fluctuation amplitude remain the same, and as long as both are uncorrelated with previous samples, the linear time dependence predicted by equation (21) holds. For completeness, Figure 1 also shows the case of "brown" noise, in which the time intervals undergo a random walk (akin to brownian motion) so that a correlation of time intervals is present; in this case, the time development of the energy is slower with $\langle E \rangle \propto t^{1/2}$ (see also MM04). Thus, the long term evolution of an ensemble of stochastic pendulums obeys the analytic expectations derived above, provided that (1) the fluctuations are independent, and (2) the long-time limit has been reached.

2.4. Fraction of Bound States

Given the time evolution of the distribution function, we can now determine the fraction of low energy states as a function of time. Here, states of the system with sufficiently low energy are bound and the pendulum oscillates — instead of circulates — so that the system is in resonance. We are thus finding an estimate of the fraction of systems that remain in resonance as a function of time, where systems leave resonance due to exposure to turbulent forcing. This treatment is approximate, and provides an upper limit to the fraction of bound states, because we allow the system to freely random walk both in and out of resonance. In the following section, we address this issue by providing a more complicated treatment.

As formulated here, the energy E is the kinetic energy, so that the criterion for the resonance to be undone (for the libration angle to circulate) is given (approximately) by $E > 1$. Note that the system must have $E > 2$ to be freely circulating, but systems with energies in the range $1 < E < 2$ have such large libration angles as to not be in a well-defined resonant state. As encapsulated in the probability distribution function for the energy, the system always has some probability of remaining in resonance, even as the mean energy $\langle E \rangle$ grows ever larger. This probability is a decreasing function of time and is given by

$$\mathcal{P}_{\text{bound}} = \left(\frac{2}{\pi D \tau} \right)^{1/2} \int_0^1 \frac{dE}{\sqrt{E}} \exp \left[-\frac{2E}{D\tau} \right] = \frac{2}{\sqrt{\pi}} \int_0^{z_0} e^{-z^2} dz = \text{Erf}(z_0) \,, \qquad (22)$$

where $z_0 = (2/D\tau)^{1/2}$. Here $\text{Erf}(z)$ is the error function (e.g., Abramowitz & Stegun 1970), which can be expanded in the limit of small z as follows:

$$\text{Erf}(z) = \frac{2}{\sqrt{\pi}} \left(z - \frac{z^3}{3} + \frac{z^5}{10} - \frac{z^7}{42} + \dots \right) \,, \qquad (23)$$
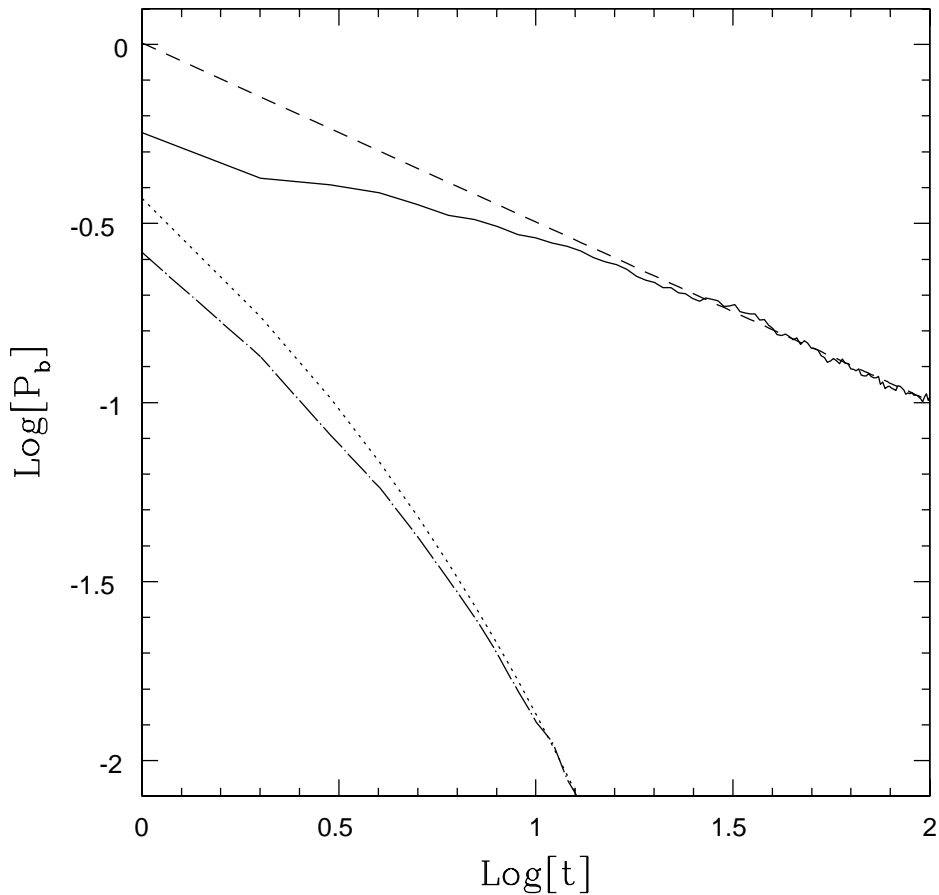
Fig. 2.— Time evolution of the probability for the planetary system to stay in a mean motion resonance as a function of time. The solid curve shows the result of 1000 realizations of the stochastic pendulum equation; in this set of numerical experiments, the system is allowed to come in and out of resonance freely. The dashed curve shows the expected asymptotic behavior of the system, i.e., a survival probability of the form $\mathcal{P}_{\mathrm{bound}} \propto t^{-1/2}$. The dot-dashed curve shows the survival probability for when a one-way barrier is imposed so that systems that leave resonance (the pendulum becomes unbound) are not allowed to re-enter the bound configuration. The dotted curve shows the analytic approximation to this probability evolution derived in the text.

where small z values correspond to late times. To leading order, the probability that the planetary system remains in resonance is thus given by the relation

$$\mathcal{P}_{\text{bound}} \approx \left(\frac{8}{\pi D \tau} \right)^{1/2} = \left(\frac{2}{\pi \langle E \rangle} \right)^{1/2} \approx \frac{8}{[\Omega t \, \langle \eta_k^2 \rangle]^{1/2}} \, . \tag{24}$$

This expression is valid only for sufficiently late times when $\tau > 2/D$. For typical migrating planets, the quantity (Ωt) is roughly the number of orbits, N_{orb}, which is expected to lie in the range $N_{\text{orb}} = 10^6 - 10^8$. This result, coupled with the expected range of $\langle \eta_k^2 \rangle$, implies that the probability $\mathcal{P}_{\text{bound}}$ of remaining in resonance lies in the range $0.001 \leq \mathcal{P}_{\text{bound}} \leq 0.08$. In other words, mean motion resonances are rare if turbulence is common, where rare means at the 1 percent level.

Equation (24) shows that the probability of a planetary system remaining in resonance should decrease as the square root of time. This dependence is observed in numerical simulations using the stochastic pendulum equation. Figure 2 shows how the probability of staying in resonance decreases with time. The solid curves shows the percentage of systems remaining in resonance as a function of time, using a sample of 10^4. The smooth dashed and dotted curves show the analytic predictions for the time dependence derived above.

This estimate of the probability for remaining bound is approximate in several respects. First, we have not included the potential energy term $(\omega_0^2 \cos \varphi)$ in the calculation of the probability distribution $P(E; \tau)$. This approximation leads to an uncertainty of $\sim \sqrt{2}$ in the estimates presented here. Next we note that the analysis presented thus far actually represents an upper limit on the fraction of systems that can remain in resonance. In the stochastic pendulum formalism, we are implicitly assuming that the system can random walk both in and out of a bound configuration, i.e., that the planetary system can random walk in and out of a resonant configuration. The model equation developed here only has one degree of freedom, so this behavior is natural. In actual planetary systems, however, other physical variables are relevant and must have the proper values to allow the planets to be in resonance. This difficulty implies that once a planetary systems leaves resonance, it will be unlikely to random walk back into resonance. This behavior, in turn, implies that the fraction of planetary systems remaining in resonance will fall below the fiducial $\mathcal{P}_{\text{bound}} \propto \tau^{-1/2}$ law. We consider this complication in the following sections.

2.5. Evolution with a One-way Barrier

The discussion presented thus far assumes that the stochastic oscillator can diffuse in and out of a bound state, i.e., into resonance as well as out of resonance. For the simple

model case, which has only one variable, this behavior is possible. For real planetary systems, however, the conditions of resonance are more complicated than the simple pendulum model. In particular, for highly interactive systems (e.g., the observed 2:1 resonance in GJ876; see §3), many orbital elements of both planets must have the proper values for the planets to be in a mean motion resonance. In such systems, while it remains possible for fluctuations to compromise the resonance, it will be unlikely for the system to random walk back into resonance. The fraction of systems that remain bound will thus decrease with time more sharply than suggested by the considerations of the previous section. As a result, the model derived above, where $\mathcal{P}_{\mathrm{bound}} \propto \tau^{-1/2}$, represents an *upper limit* on the fraction of systems that remain in resonance. In this section, we explore a more complicated model for the probability evolution that includes the one-way nature of this process. We also consider the intermediate case of a partically transmitting barrier, where systems can return to resonance after leaving, but with reduced probability.

2.5.1. Heuristic Model Equation

We now consider a simple generalization of the time evolution of the probability. At any given time, the fraction of systems that would remain bound in the absence of the one-way barrier is given by $\mathcal{P}_{\mathrm{bound}}$ from equation (24). We then assume that some fraction of these systems are "lost" at a well-defined rate, so that the time evolution of the fraction of bound states (in the absence of the diffusion term) would be an exponential decay. This ansatz thus assumes that the remaining systems are distributed across the possible bound energy values, and that each system has some probability of leaving its bound state per unit time. With this assumption, the Fokker-Planck equation for the averaged probability distribution function $p(V; \tau)$ now takes the modified form

$$\frac{\partial p}{\partial \tau} = \frac{D}{4} \frac{\partial^2 p}{\partial V^2} - \gamma \left(\frac{8}{\pi D \tau} \right)^{1/2} p \, , \tag{25}$$

where we assume that the bound fraction has the asymptotic form derived above and where the parameter γ encapsulates the details of this "decay process". This equation can be solved to obtain the result:

$$p(V; \tau) = \frac{1}{(\pi D \tau)^{1/2}} \exp\left[-\frac{V^2}{D\tau} \right] \exp\left[-\gamma \left(\frac{32\tau}{\pi D} \right)^{1/2} \right] \, . \tag{26}$$

With this complication, the fraction of systems that remain bound as a function of time now takes the form

$$\mathcal{P}_{\mathrm{bound}} \approx \left(\frac{8}{\pi D \tau} \right)^{1/2} \exp\left[-\gamma \left(\frac{32\tau}{\pi D} \right)^{1/2} \right] \, . \tag{27}$$

Although heuristic, this model captures the basic time behavior for stochastic pendulums with a one-way barrier, as shown in Figure 2.

2.5.2. Solutions from Separation of Variables

For the simplest case of a constant diffusion constant, the solution for a one-way barrier can be found using separation of variables. In this case, the solution to the diffusion equation is assumed to have the general form $p(t, V) = T(t)g(V)$; the diffusion equation then can be written as

$$\frac{1}{T}\frac{dT}{dt}\frac{4}{D} = \frac{1}{g}\frac{d^2g}{dV^2} = -\Lambda^2 \,, \tag{28}$$

where Λ^2 is the separation constant.

The solutions $g(V)$ have the form

$$g_n(V) = A_n \cos \Lambda_n V \,, \tag{29}$$

where the subscript denotes one of a series of solutions that satisfy the boundary condition. We we invoke the boundary condition that $g(V = \sqrt{2}) = 0$, which implies that the distribution function vanishes when the kinetic energy reaches $E = V^2/2 = 1$. This condition thus specifies the eigenvalues Λ_n, i.e.,

$$\Lambda_n = \frac{\pi}{\sqrt{2}}(n + 1/2) \,, \tag{30}$$

where n is an integer. The full solution thus takes the form

$$p(t, V) = \sum_{n=0}^{\infty} A_n \cos(\Lambda_n V) \exp\left[-\frac{1}{4}D\Lambda_n^2 t\right] \,. \tag{31}$$

For the initial condition $p(t = 0, V) = \delta(V)$, where $\delta(x)$ is the Dirac delta function, the constants are specified so that

$$A_n = 1/\sqrt{2} \,. \tag{32}$$

The fraction of bound states at any time is then given by

$$\mathcal{P}_{\text{bound}} = 2 \int_0^{\sqrt{2}} p(t, V)dV = \sum_{n=0}^{\infty} \frac{2(-1)^n}{\pi(n + 1/2)} \exp\left[-\frac{D}{8}\pi^2(n + 1/2)^2 t\right] \,. \tag{33}$$

This solution, though approximate, indicates that the long term evolution of the ensemble of resonant states follows an exponential decay. For the simple solution of equation (31), each "mode" decays exponentially, albeit with a differing decay rate. In the long run, however, only the lowest order mode survives, and the time evolution becomes purely exponential.

2.5.3.   Further Complications

The evolution of the actual stochastic pendulum differs from that described by a simple diffusion equation in several respects. Most importantly, the diffusion constant D is not really a constant. In the formulation developed here, $D \propto \sin^2 \varphi$, and we have taken the average value $\langle \sin^2 \varphi \rangle = 1/2$. However, this limit only applies in the long time limit when most of the oscillators in the ensemble have large energy, so that their angles uniformly sample the possible values. For bound states, by definition, the energies are low, and hence this limiting form is not strictly applicable. In particular, the typical amplitudes of the bound oscillators will be smaller than average, and the true effective diffusion constant will be less than that of the long time limit. In addition to its lower value, the diffusion constant will also have some type of time dependence: In the beginning, when all of the oscillators in the ensemble have small amplitudes, D will be correspondingly small. As time increases, even the bound oscillators will have larger amplitudes and hence the evolution is properly described by larger values of D (but still smaller than that of the long time limit).

2.5.4.   Partial Barriers

As shown above, the time evolution of the number of bound states decays exponentially for systems with a strict one-way barrier, i.e., for the case in which systems that leave resonance are not allowed to return. We now consider the case in which a given system has some probability $\rho_{\rm ret}$ of re-entering a bound (resonant) state after leaving, where $0 \leq \rho_{\rm ret} \leq 1$. In this case, all of the systems are allowed to stay in play, but only a fraction of the systems can make the transition from an unbound state to a bound state. As shown below, even when the fraction $\rho_{\rm ret} \ll 1$, this modification makes a large qualitative change in the long-term behavior of the system.

We first note that at late times, essentially all of the bound states in the original problem (without a barrier) are those that have returned to resonance after leaving. This claim follows directly from the above results: The fraction of bound states of all types decreases as $\sim t^{-1/2}$, while the fraction of bound states that have never left resonance decreases as $\sim \exp[-\gamma t]$, where the decay rate γ depends on the details of the diffusion process. At late times, however, the power-law behavior wins, and hence most bound states are due to systems that have returned from higher energy states. If the higher energy states are allowed to re-enter resonance with probability $\rho_{\rm ret}$, then the fraction of systems in a resonant state will again follow the $t^{-1/2}$ law, but with a smaller normalization. Specifically, the normalization is reduced by the factor $\rho_{\rm ret}$ and the long-term solution for the fraction of bound states

becomes

$$\mathcal{P}_{\text{bound}} \approx \rho_{\text{ret}} \left(\frac{8}{\pi D \tau} \right)^{1/2} . \tag{34}$$

This behavior is illustrated in Figure 3, which shows the time evolution for an ensemble of stochastic pendulums. The upper two curves show the evolution for the case in which the systems can freely re-enter a resonant (bound) state after leaving. The bottom two curves show the fraction of bound states for the case in which the systems are allowed to have only a 20% probability of returning to resonance after leaving. The solid and dashed curves show the results of the actual numerical integrations, whereas the dotted curves show the analytic approximations derived above. Notice the good agreement between the predicted asymptotic forms and the numerical results. The fluctuations of the numerically determined fractions about the analytic predictions have amplitudes that are consistent with $\sqrt{N}$ noise; note that the numerical ensemble contains only 10^4 systems and the number of bound states is much smaller by the end of the time interval shown in Figure 3.

On a related note, one can consider the problem in which systems leaving a bound state have some probability p_X of never returning to resonance. Perhaps surprisingly, the long term behavior for this case is wildly different than for the previous case. Here, for any nonzero value of p_X, the time dependence of the number of bound states is always an exponential decay.

2.6.   Other Resonances

As outlined above, the 2:1 resonance is generally the strongest, and planets in such a configuration should survive longest in the presence of turbulence. For other resonances, the oscillation frequencies are generally smaller so that the periods of libration are longer. For the case of the 3:1 resonance, for example, ones finds (MD99) that

$$\omega_0^2 \approx -0.8636 \mu \Omega^2 e^2 . \tag{35}$$

The negative sign indicates that the stable equilibrium point of the oscillator occurs at $\varphi = \pi$ rather than $\varphi = 0$. After defining $\phi \equiv \varphi - \pi$, the equation of motion for ϕ becomes the same as before. The above frequency is thus lower than that of the (simplified) 2:1 resonance by a factor of $\sim (3/e)^{1/2}$. The potential energy of the oscillator is thus less deep by a factor $3/e$, about 30 for typical cases, so that the system is more easily bounced out of a resonant state by turbulence.

In order to assess the probability of remaining in a bound (resonant) configuration, one can evaluate the equations derived in §2.3 – 2.5 using the proper frequency given by equation
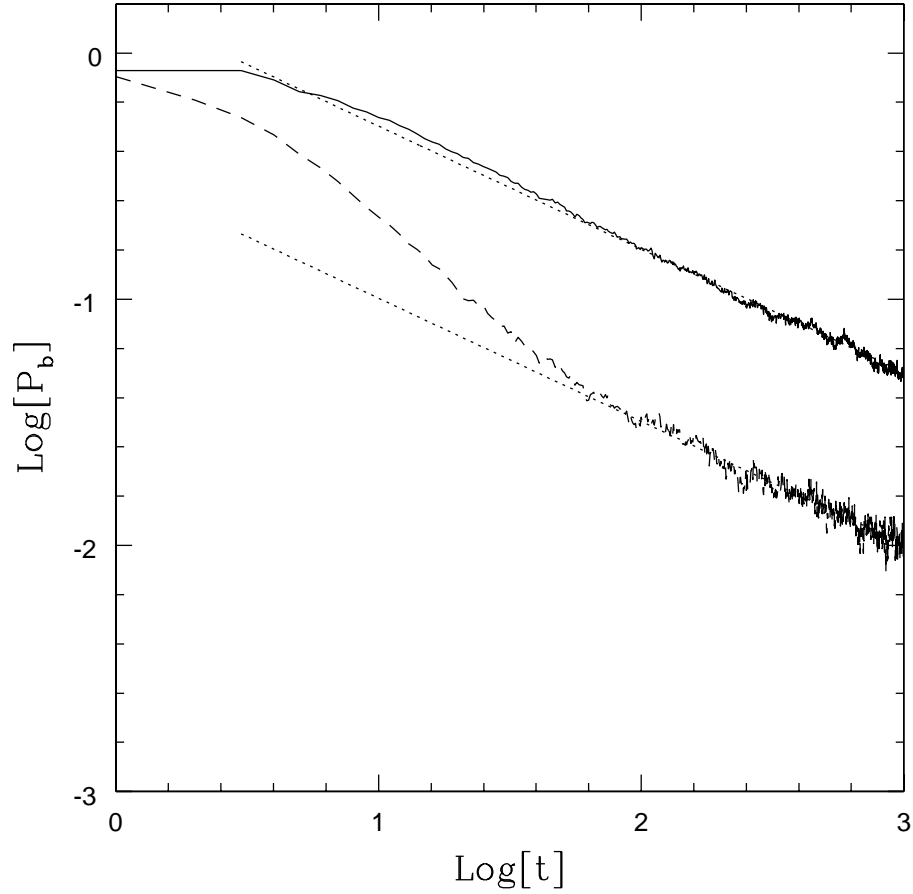
Fig. 3.— Time evolution of the fraction of planetary systems that stay in a mean motion resonance as a function of time. The solid and dashed curves show the result of 10,000 realizations of the stochastic pendulum equation. For the top (solid) curve, the system is allowed to come in and out of resonance freely; for the bottom (dashed) curve, the system has only a 20% chance of returning to a bound state after leaving. The two dotted curves shows the expected asymptotic behavior of the system, i.e., a survival probability of the form $\mathcal{P}_{\mathrm{bound}} \propto t^{-1/2}$.

(35). For example, the resulting estimate for the probability of remaining in resonance has the form of equation (24), with the leading coefficient smaller by a factor of $3/e \sim 30$. In other words, at any given time, the probability of a planetary system remaining in a mean motion resonance, in the face of turbulence, is inversely proportional to the relevant value of ω_0^2. For typical values of the orbital elements of extrasolar planets, where $e \sim 0.1$, the probability of staying in a 3:1 mean motion resonance is about 30 times smaller than for a 2:1 resonance.

2.7. Model Summary

The basic analytical model developed here contains three physical variables that describe the effects of turbulent perturbations on mean motion resonance. The first variable is the natural oscillation frequency ω_0 of the resonance (§2.1), modeled here as a pendulum; this quantity represents the oscillation frequency of the libration angle in the planetary system. The time scale associated with this frequency is typically ~ 100 times longer than the orbital time scale of the planets, and depends on the system properties in a well-known manner (see §2.1 and MD99). The second variable is the time scale $\Delta t \approx 8\pi/\Omega$ (or its dimensionless counterpart $\Delta\tau \approx 8\pi\omega_0/\Omega$) over which the turbulent perturbations are re-established to provide an independent realization of the torques. The final variable is the amplitude of the perturbations. Since the torques and their corresponding changes in angular momentum can be either positive or negative, and hence the mean vanishes, the perturbation amplitude can be characterized by the root mean square $j_{\rm rms} = \langle (\Delta J)^2/J^2 \rangle^{1/2}$; this quantity also has a dimensionless counterpart $\eta_{\rm rms}$ given by equations (13) and (14). Numerical simulations of MHD turbulence indicates that the amplitude lies in the range $5 \times 10^{-5} < j_{\rm rms} < 2 \times 10^{-2}$.

For the simplest version of this model, where systems can freely random walk back into a resonant state, the three variables $(\omega_0, \Delta t, \eta_{\rm rms})$ determine the long term evolution of the ensemble. In particular, the expectation value of pendulum energy increases linearly with time according to equation (21). The probability of the system staying (bound) in resonance decreases as the square root of time according to equation (24). Note that both of these results depend only on the dimensionless time $\tau = \omega_0 t$ and a dimensionless diffusion constant $\mathcal{D} = \eta_{\rm rms}^2/\Delta\tau$. In other words, the action of the turbulent fluctuations can be described by a diffusion constant that determines how the variables of the system – considered here as a nonlinear oscillator – random walk through phase space.

In more complicated versions of the model, where systems cannot easily return to a resonant state, the long term behavior results is a lower probability of remaining bound. As a result, the simple result described above provides an upper limit on the expected number

of resonant states as a function of time. In the opposite limit in which systems that leave resonance can never return, the number of bound states decays exponentially, with varying decay rates, as indicated by equations (27) and (31). For the case in which systems can re-enter resonance after leaving, but with reduced probability, the number of bound states decreases as $t^{-1/2}$ as before, but with reduced normalization, as shown by equation (34).

3. NUMERICAL SIMULATIONS

In this section, we consider an ensemble of numerical integrations motivated by an observed extrasolar planetary system. For this exploration, we adopt the outer planets c ($P \sim 60$ d) and b ($P \sim 30$ d) of the Gliese 876 planetary system (Marcy et al. 2001). These planets are observed to lie deep in the 2:1 mean motion resonance, with the angles θ_1 and θ_2 librating with small amplitudes (Laughlin& Chambers 2001, Rivera et al. 2005). Indeed, Gliese 876 b and c represent, by far, the most convincing case of an extrasolar planetary system in mean motion resonance. Among the 25 multiple-planet systems that have been discovered to date, 2:1 mean motion resonances have also been tentatively identified for HD 82943 b and c (Gozdziewski & Maciejewski 2001, Mayor et al. 2004, Lee et al. 2006), HD 128311 b and c (Vogt et al. 2005), and HD 73526 b and c (Tinney et al. 2005). In each of these three cases, however, the libration widths of the resonant arguments are very uncertain, and for HD 128311 and HD 73526, the best dynamical fit to the radial velocity data shows only a single argument in libration. Following the discovery of 55 Cancri c and d (Marcy et al. 2002), it was suggested by several authors (e.g., Ji et al. 2003) that 55 Cancri b and c are possibly participating in a 3:1 mean motion resonance. Self-consistent 6-body fits to the 55 Cancri data set published by Fischer et al. (2007), however, show no evidence that 55 Cancri b and c are in 3:1 resonance.[1]

In this set of numerical experiments, we start an ensemble of planetary systems with the observationally determined orbital elements of GJ876, so that the system begins in a 2:1 mean motion resonance, and then integrate the system forward in time. The integrations include additional stochastic fluctuations, which would be present if the circumstellar disk that formed the planets were still present. We then monitor how easily the system is knocked out of its resonant configuration. The ensemble of numerical integrations reported here are thus analogous to those done in the previous section with the stochastic pendulum. In this case, however, we integrate the full 18 phase space variables (6 orbital elements for each

---

[1]For an up-to-date χ^2-ranked list of self-consistent fits to the 55 Cnc data sets see http://oklo.org?p=257 and the links therein.

planet and 6 more for the star) instead of only one variable (φ) for the pendulum model. For this system, integrating the motion of the star is important because its mass is relatively small, only 0.32 $M_\odot$, whereas the masses of the planets are 0.79 and 2.53 m_J, and hence the system is highly interactive (Laughlin & Chambers 2001). As a result, the GJ876 system is as far from the idealized (one variable) model of the stochastic pendulum as any planetary system observed to date; as a result, any agreement found between the simple model and the full integrations can be considered robust.

The starting orbital elements are taken to be those observed (Rivera et al. 2005) at the present day; specifically, the epoch for the initial conditions is JD 2449679.6316, the date for which the first published Lick Observatory radial velocity was made. The systems are then integrated into the future for 2×10^4 years. Since the planets in this particular system have relatively short periods (60.830 days and 30.455 days for the outer and inner planets, respectively), the number of orbits is large – about 2.4×10^5 orbits of the inner planet. The integrations are performed with a Bulirsch-Stoer (B-S) integration scheme (e.g., Press et al. 1992) to obtain high accuracy with reasonable computational speed. In the absence of turbulent forcing, the system can be integrated forward in time for millions of years and is found to stay in resonance, where we use the following definitions for the libration angles:

$$\theta_1 = \lambda_1 - 2\lambda_2 + 2(\varpi_1 - \varpi_2) \qquad \text{and} \qquad \theta_2 = \lambda_1 - 2\lambda_2 + 2(\varpi_1 - \varpi_2), \qquad (36)$$

where the λ_j are the mean longitudes and the ϖ_j are the longitudes of periapse of the two planets. Note these angles are defined to be a linear combination of the stanard ones (e.g., Lee & Peale 2002), and are chosen because they provide a cleaner separation of the apsidal libration and the mean motions (J. Chambers, private communication). We measure the degree of resonance by monitoring the maximum amplitude of these libration angles over a given interval of time. For this purpose, we use a fixed monitoring time of 100 years, which is much longer than the period of the oscillations of the resonance, about 3.5 years, so that many oscillation periods are included in the determination of the maximum. This maximum libration angle is then tracked as a function of time. For the sake of definiteness, we consider the systems to be bound (in resonance) when the maximum angle remains less than $\theta_* = 90$ degrees; when the maximum angle exceeds $\theta_* = 90$ degrees, we consider the resonance to be compromised. Note that the exact number of bound (resonant) states as a function of time depends on the choice of the angular threshold value θ_*; however, the general trends (shown below) are qualitatively similar for any choice of threshold angle in the range $90 \leq \theta_* \leq 175$.

The effects of turbulence are introduced by adding small velocity perturbations at regular time intervals. For the sake of definiteness, we take the forcing time interval to be 1/3 yr, which is about four times the period of the inner planet, and is consistent with the time required for the turbulent torques to be independent (LSA) and with the model equations

of §2. In terms of the simple pendulum model of the system, variations of the stochastic forcing times could be scaled out of the problem (Appendeix A) and would effectively add width to the distribution of forcing strengths. In these experiments, we take the size of the velocity perturbations to have the form $\Delta v = v_A \xi$, where the amplitude $v_A = 0.0032 \; \mathrm{km/s^2}$, and where ξ is a uniformly distributed random variable on the interval $-1 \leq \xi \leq 1$. Both the $\hat{x}$ and $\hat{y}$ components of the velocity are perturbed (independently) in this manner, but the vertical velocity component is left unchanged. Including both components of the velocity perturbation, we find that the fractional change in speed, and hence angular momentum, has amplitude $[(\Delta J)/J]_k \approx 10^{-4}$, which is somewhat smaller than the benchmark value of equation (9), but well within the expected range of possible values given by equation (14).

The results from one ensemble of simulations are shown in Figures 4 and 5. Figure 4 shows the time evolution of the maximum libration angle (as defined above) for five different trials, i.e., five different realizations of the turbulent fluctuations. Note that the systems can re-enter bound states – defined here to be maximum libration angles less then $\theta_* = 90$ degrees – after leaving. Nonetheless, the results show a clear trend for systems to preferentially leave resonance, rather than return, so the number of bound states decreases rapidly with time.

We have performed an ensemble of 900 integrations of the system, where each numerical experiment uses a different realization of the stochastic perturbations due to turbulence (with this sample size, root-N fluctuations are $\sim 1/30 \sim 0.03$). Figure 5 shows the fraction of bound states as a function of time. The solid and dot-dashed curves show the fraction of systems that remain in resonance as a function of time (in years) for the first and second resonance angles, respectively. The dotted curves shows the corresponding fraction of bound states that would remain if the systems that leave resonance could never return to a bound state. These results clearly indicate that the actual fraction of bound states is systematically larger than the fraction of bound states that would result if systems were never allowed to return to a resonant state after leaving (compare the dotted and solid curves in Figure 5). In other words, planetary systems can — sometimes — random walk back into a resonant configuration after leaving. This behavior is consistent with that found for the evolution of individual systems (shown in Fig. 4). Finally, the dashed curve shows the power-law behavior $\mathcal{P}_{\mathrm{bound}} \propto t^{-1/2}$ for reference. Note that the time evolution of the fraction of bound states falls below the prediction of a pure power-law with $\mathcal{P}_{\mathrm{bound}} \sim t^{-1/2}$. The long term behavior of the number of bound states seems to follow a steeper power-law, but does reach a full expenential decay during the time window studied (which would be expected if systems never return to resonance).

---

[2]This amplitude value was chosen to be a round number, namely 2×10^{-4}, in code units, where $G = 1$, mass is measured in $M_\odot$, and time is measured in years.
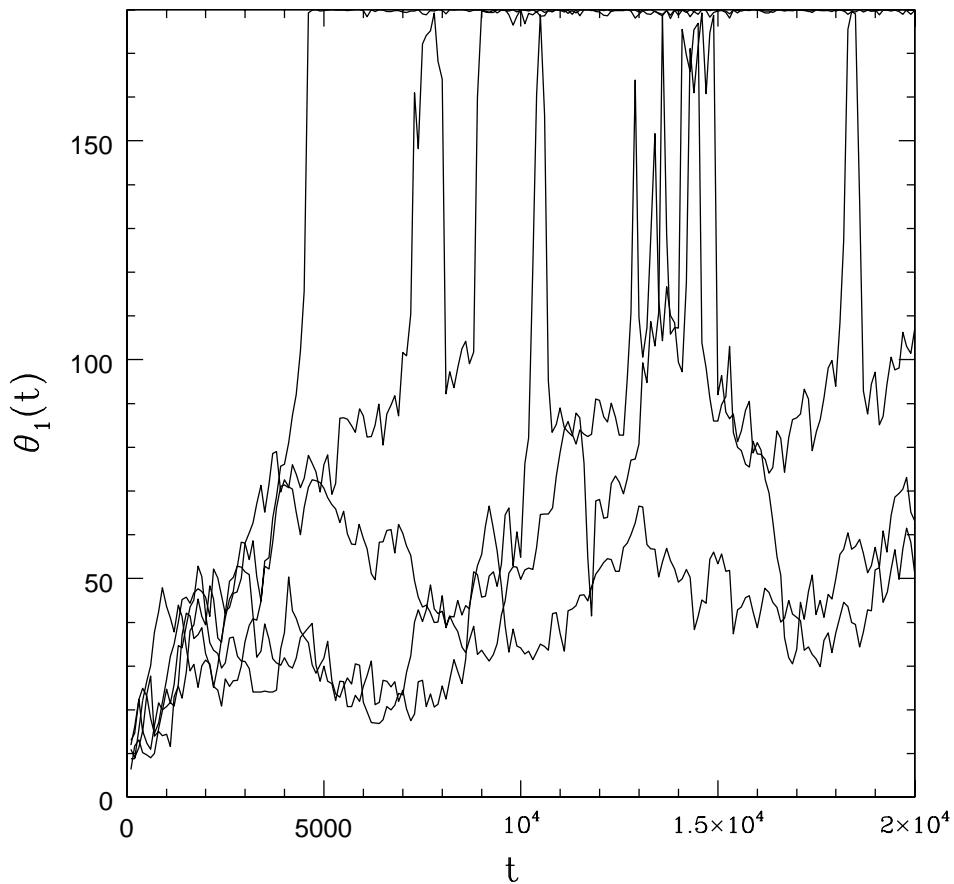
Fig. 4.— Time evolution of the resonance angles for a collection of planetary systems based on the observed system GJ876. The systems are subjected to turbulent forcing as described in the text. The five curves show the first resonance angle θ_1 as a function of time (given here in years) for the five different realizations of the turbulent fluctuations.
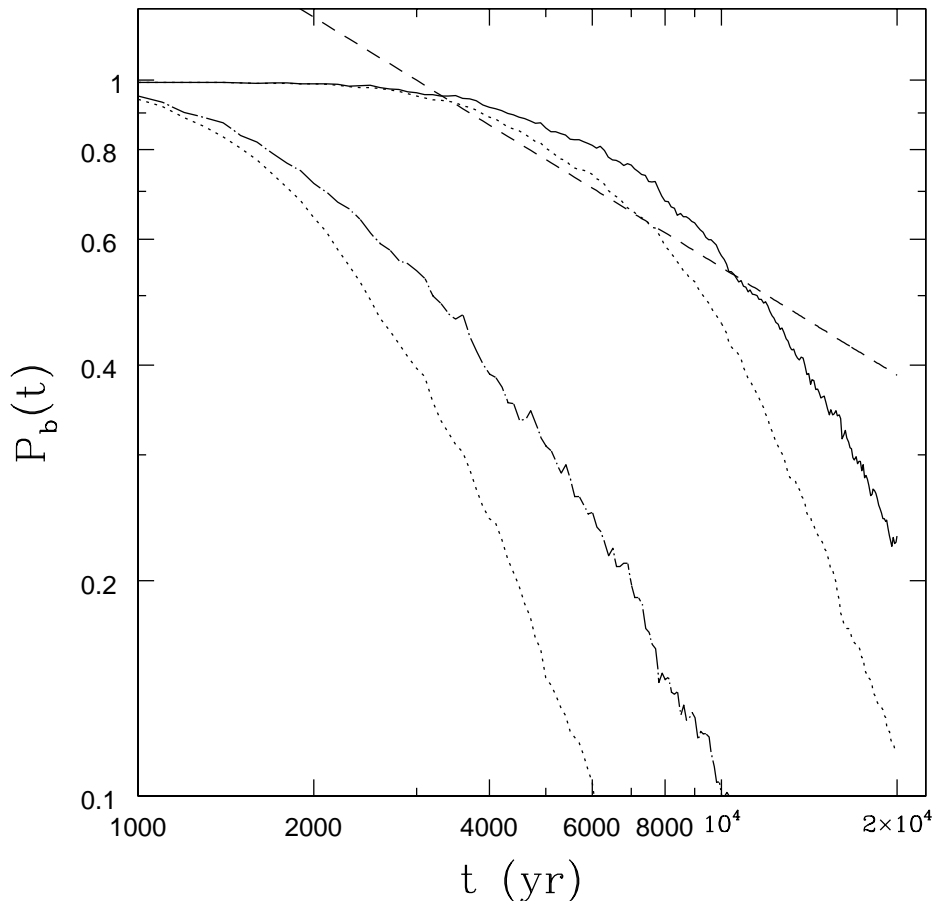
Fig. 5.— Time evolution of the fraction of bound states, as measured by the maximum excursions of the resonance angles, for a collection of planetary systems based on the observed system GJ876. The systems are subjected to turbulent forcing as described in the text. The solid and dot-dashed curves show the fraction of systems that remain in resonance as a function of time (in years) for the first and second resonance angles, respectively. The dotted curve shows the fraction of bound states for the first resonance angle that would result if systems that leave resonance could never return to a bound state. For reference, the dashed curve shows the power-law behavior $P \propto t^{-1/2}$ expected for a simple stochastic pendulum.

As an order of magnitude check on the time scales, note that the fractional change in velocity per stochastic kick has amplitude $\Delta v \sim 10^{-4} v_{orb}$, where v_{orb} is the orbital speed of the inner planet. As outlined in §2, however, the energy associated with the potential well of the resonance is much smaller than that of orbit. If we denote the change in velocity required to leave resonance as v_{res}, then $v_{res} \sim 0.01 v_{orb}$, which in turn implies $\Delta v \sim 0.01 v_{res}$. If Δv accumulates as a random walk, the system thus requires $\sim 10^4$ stochastic forcing kicks to account for enough energy to compromise resonance, and this number translates into a time scale of ~ 3000 yr. Indeed, individual systems (see Fig. 4) and the ensemble (see Fig. 5) evolve on a comparable time scale.

4.   DISCUSSION AND CONCLUSION

The main finding of this paper is that mean motion resonance in planetary systems is readily compromised through the action of turbulent fluctuations in circumstellar disks. If MRI operates and the accompanying turbulent torques are common during the epoch of planetary migration, then planetary systems in mean motion resonances are predicted to be rare. Specifically, even for the most favorable case in which the system can freely random walk in and out of resonance, only a small percentage of the solar systems that produce pairs of planets in a resonant configuration will remain in resonance over typical disk lifetimes of ~ 1 Myr if turbulence is present. On the other hand, if planetary systems in mean motion resonance are found to be common, then this analysis implies that turbulence, and hence MRI, would have a severely limited duty cycle.

We have addressed this problem using both direct numerical integrations of sample solar systems and through the construction of model equations that represent an ensemble of stochastically driven pendulums. This latter approach allows for the derivation of a number of analytic results that elucidate the basic physics of solar systems being driven from their resonant states by turbulent forcing. For this class of systems, the energy of the ensemble of stochastic oscillators increases linearly with time (see Fig. 1, eq. [21], and Appendix B), the distribution of energy for the ensemble spreads according to the solution of equation (20), and the probability of a planetary system remaining in resonance decreases as $t^{-1/2}$ (see Fig. 2). This law holds both for the case in which systems can freely re-enter resonance, and for the case in which they re-enter resonance with a given (fixed) probability, although the normalization is lower for the latter case (eq. [34]). If systems that leave resonance can never return to a bound state, then the time evolution of the fraction of bound states is a decaying exponential (§2.5).

The results from our numerical integrations indicate that the fully interactive system

(with 18 phase space variables) behaves in a qualitatively similar manner to the stochastic pendulum (with one variable). In particular, the number of bound states (systems in resonance) decreases with time, where the evolution of the ensemble of systems is diffusive, and where the diffusion constant depends on the square of the fluctuation amplitude and inversely on the time scale of the turbulent forcing. The resulting function that decribes the decrease in the number of resonant states is intermediate between the $t^{-1/2}$ power-law behavior of the simplest pendulum system and the decaying exponential form that applies for systems that can never re-enter resonance after becoming unbound. The numerical simulations show that systems can indeed random walk back into a resonant state after leaving, consistent with the finding that the number of bound states does not decay exponentially. On the other hand, the return to resonance is relatively rare, in particular more unlikely than for the (one variable) stochastic pendulum, a result that is consistent with the fraction of bound states falling below the $t^{-1/2}$ law. This latter power-law behavior — the solution to the the long term behavior of a stochastic pendulum – thus provides an upper limit on the probability of resonant states as a function of time.

The most important astronomical implication of this work is a quantitative determination of the rarity of solar systems surviving in a resonant configuration. Our results can be summarized by the following expression, which represents our upper bound on the fraction of surviving bound (resonant) states:

$$\mathcal{P}_{\text{bound}} = \frac{\rho_{\text{ret}}}{\eta_{\text{rms}}} \left(\frac{32}{\pi N_{\text{orb}}} \right)^{1/2} \equiv \frac{C}{N_{\text{orb}}^{1/2}} , \tag{37}$$

where ρ_{ret} is the probability of returning to resonance, η_{rms} is set by the amplitude of the fluctuations, and N_{orb} is the number of orbits over which the turbulence is active. In the second equality we have defined the dimensionless quantity $C = (32/\pi)^{1/2} \rho_{\text{ret}}/\eta_{\text{rms}}$. For typical turbulent amplitudes, $\eta_{\text{rms}} \approx 0.13$, and hence $C \approx 25\rho_{\text{ret}}$. Given that returning to resonance requires somewhat special conditions, so that ρ_{ret} is generally small, we expect the parameter C to be of order unity. Since $\rho_{\text{ret}} \leq 1$, by definition, we can also find a more conservative, but more rigorous, upper bound on the fraction of surviving resonant systems, $\mathcal{P}_{\text{bound}} < 25N_{\text{orb}}^{-1/2}$, which has a value of ~ 0.025 for a typical value of $N_{\text{orb}} = 10^6$.

In addition to the prediction that resonant states are rare, this work has other astronomical implications: For the particular case of the Gliese 876 system, if no eccentricity damping is assumed for the epoch of planet formation and migration, then the current eccentricities and libration widths of the system suggest that the system migrated only a small distance (8% of the initial semi-major axes) while in resonance (Lee & Peale 2002). This result is consistent with any turbulence in the disk of the GJ876 system having had little time or ability to provide substantial perturbations on the resonant arguments. On the other hand,

the observed HD 128311, HD 82943 and HD73526 planetary systems are all consistent with having received significant exposure to turbulent perturbations, but not enough to have destroyed their librations completely. Once a large sample of multiple-planet systems has been assembled, we should gain further insight from the distribution of observed resonant widths, in addition to the observed fraction of planets in mean motion resonance. In particular, if planets can random walk back into the resonance after leaving, as indicated by both our numerical integrations and model equations, the observational sample should show a definite preference for systems with large libration widths. This trend is exactly what we observe for the tenuous resonances in the three systems other than Gliese 876.

This analysis also outlines the basic physical mechanism by which turbulence affects mean motion resonance. We have modeled the process through a pendulum equation (which represents the resonance) with the addition of stochastic forcing (which represents the turbulence). This analysis applies specifically to the class of systems for which the turbulent fluctuations provide forcing kicks that are fully independent, i.e., where both the amplitude of the fluctuations and the time intervals are not correlated. In this case, the results are largely independent of the distributions, and depend primarily on the expectation values of the amplitudes and time intervals of the turbulent forcing; these latter quantities set the value of the effective diffusion constant in the problem. This behavior is analogous to that found earlier for the problem of turbulent fluctuations affecting the rate of ambipolar diffusion in molecular clouds cores (Fatuzzo & Adams 2002).

Note that the effective diffusion constant $D \propto (\Delta J)_k^2/(\Delta t)_k$. In order to set the proper value of the constant D, one must choose the time interval to be long enough so that the fluctuations are independent and short enough that the changes in angular momentum (ΔJ) increase linearly with time (where we now suppress the index k). Suppose, for example, one were to choose a longer time interval to sample the fluctuations, say $(\Delta t) \gg (\Delta t)_0$, where $(\Delta t)_0$ is the time interval for optimal sampling. The change in angular momentum over one sampling interval would then increase as a random walk (even within the time interval), i.e., $(\Delta J) = (\Delta J)_0[(\Delta t)/(\Delta t)_0]^{1/2}$. The effective value of the diffusion constant then scales according to $D \propto (\Delta J)^2/(\Delta t) = (\Delta J)_0^2[(\Delta t)/(\Delta t)_0]/(\Delta t) = (\Delta J)_0^2/(\Delta t)_0$. We thus recover the correct value, provided that the changes in angular momentum are computed properly. In this paper, we have taken the time interval Δt to be four times the orbital period of the inner planet (twice the period of the outer planet), consistent with the calculations of LSA (see also Nelson 2005). The above considerations imply that the diffusion constant D is linearly proportional to Δt, and the fraction of bound states scales as $D^{-1/2}$, so that our quoted results are only weakly dependent on any uncertainty/error in the specification of Δt.

Although our general conclusion is robust – namely, that turbulence easily compromises mean motion resonances – a good deal of additional work should be carried out. This treatment assumes that the planets have already formed, and have already migrated to their (nearly) final radial locations, and then considers the effects of turbulence on mean motion resonances. In actuality, planets can be subjected to turbulent fluctuations as they migrate inward and become locked into resonance. These processes of planet formation, migration, resonance locking, and turbulent forcing should thus be studied concurrently. In addition, the differences between the results of our full numerical integrations (which include all 18 phase space variables of the system) and those of the idealized stochastic pendlum (which has only one degree of freedom) poses a mathematically interesting issue for further study.

APPENDIX A: RESCALING FOR VARIABLE TIME INTERVALS

In this Appendix, we show that if the stochastic forcing impulses occur at irregular time intervals, then the time variable can be rescaled to make the stochastic forcing kicks occur at regular (periodic) intervals. As a compensating result, however, the distribution of the forcing strengths becomes wider and the natural oscillation frequency of the system takes on a distribution of values.

We begin by writing the stochastic pendulum equation in the form

$$\frac{d^2\varphi}{dt^2} + \left[\omega_0^2 + q_k Q(\lambda_k t)\right] \sin\varphi = 0\,, \tag{A1}$$

where Q is a periodic function and q_k determines the forcing strength for the kth time interval; the variable λ_k has unit mean, but allows for different time intervals for the stochastic forcing terms. Notice that we generally use periodic Dirac-delta functions to specify the forcing time,

but this argument can be generalized to include any periodic function Q. If we re-scale the time variable for each cycle according to

$$t \to \lambda_k t \,, \tag{A2}$$

then the stochastic pendulum equation takes the form

$$\lambda^2 \frac{d^2\varphi}{dt^2} + \left[\omega_0^2 + q_k Q(t)\right] \sin\varphi = 0 \,, \tag{A3}$$

where the time variable appearing in this equation is the rescaled one. If we then re-scale the remaining parameters (ω_0, q_k) according to the relations

$$\omega_0 \to \omega_0/\lambda_k \equiv \omega_k \qquad \text{and} \qquad q_k \to q_k/\lambda_k^2 \equiv \tilde{q}_k \,, \tag{A4}$$

the stochastic pendulum equation has the same form as that for the case of perfectly periodic forcings. This result is thus the analog of Theorem 1 of Adams & Bloch (2008) for the stochastic Hill's equation. Notice that in this case the forcing strength q_k acquires a new (generally wider) distribution to accommodate the variation in forcing periods, and, the natural oscillation frequency ω_0 becomes a random variable.

APPENDIX B: ALTERNATE DERIVATION OF THE LINEAR TIME DEPENDENCE FOR THE MEAN ENERGY

In this Appendix, we present an alternate derivation of the result that the energy of a stochastically driven pendulum tends to increase linearly with time (in the limit of long times). This result is thus consistent with equation (21) in the text.

We begin by considering the pendulum equation with a periodic delta-function forcing term, as described in the text (§2). The angle φ itself must be continuous at the moment of forcing, but the derivative of φ obeys a jump condition that can be written in the form

$$\left.\frac{d\varphi}{d\tau}\right|_+ = \left.\frac{d\varphi}{d\tau}\right|_- - q_k \sin\varphi_k \,, \tag{B1}$$

where we have denoted the value of the angle at the *kth* cycle boundary as φ_k. Since the angle φ must be a continuous function across the boundary, the potential energy is also a continuous function, and hence the total energy experiences discrete jumps of the form

$$\Delta E = -q_k \sin\varphi_k \left.\frac{d\varphi}{d\tau}\right|_- + \frac{1}{2} q_k^2 \sin^2\varphi_k \,. \tag{B2}$$

Over long times, the first term in the above equation averages to zero, whereas the second term averages to $\langle q_k^2 \rangle / 4$. The mean energy thus grows as

$$E \approx \frac{\langle q_k^2 \rangle}{4\Delta\tau}\tau\,, \tag{B3}$$

where Δt is the time interval of the stochastic forcing. Not only does this argument reproduce the linear growth of the mean energy, as found using the Fokker-Planck analysis in the text, but it also results in the same coefficient if we identify the effective diffusion constant $D = \langle q_k^2 \rangle / (\Delta\tau)$.

REFERENCES

Abramowitz, M., & Stegun, I. A. 1970, Handbook of Mathematical Functions (New York: Dover)

Adams, F. C., & Bloch, A. M. 2008, SIAM J. Appl. Math., in press

Balbus, S. A., & Hawley, J. F. 1991, ApJ, 376, 214

Beaugé, C., Michtchenko, T. A., Ferraz-Mello, S. 2006, MNRAS, 365, 1160

Binney, J., & Tremaine, S. 1987, Galactic Dynamics (Princeton: Princeton Univ. Press)

Butler, P. R., et al. 2006, ApJ, 646, 502

Fatuzzo, M., & Adams, F. C. 2002, ApJ, 570, 210

Fatuzzo, M., Adams, F. C., & Melia, F. 2006, ApJ, 653, L49

Fischer, D. A., et al. 2007, ArXiv e-prints, 712, arXiv:0712.3917

Goździewski, K., & Maciejewski, A. J. 2001, ApJ, 563, L81

Ji, J., Kinoshita, H., Liu, L., & Li, G. 2003, ApJ, 585, L139

Holman, M. J., & Murray, N. W. 1996, AJ, 112, 1278

Johnson, E. T., Goodman, J., & Menou, K. 2006, ApJ, 647, 1413

Laughlin, G., & Chambers, J. E. 2001, ApJ, 551, 109

Laughlin, G., Steinacker, A., & Adams, F. C. 2004, ApJ, 608, 489 (LSA)

Lee, M. H. 2004, ApJ, 611, 517

Lee, M. H., & Peale, S. J. 2002, ApJ, 567, 596

Lee, M. H., Butler, R. P., Fischer, D. A., Marcy, G. W., & Vogt, S. S. 2006, ApJ, 641, 1178

Mallick, K., & Marcq, P. 2004, J. Phys. A, 37, 4769 (MM04)

Marcy, G. W., Butler, R. P., Fischer, D., Vogt, S. S., Lissauer, J. J., & Rivera, E. J. 2001, ApJ, 556, 296

Marcy, G. W., Butler, R. P., Fischer, D., Laughlin, G., Vogt, S. S., Henry, G. W., & Pourbaix, D. 2002, ApJ, 581, 1375

Mayor, M. et al. 2001, ESO Press Release 07/01

Mayor, M. et al. 2004, A & A, 415, 391

Moorhead, A. V., & Adams, F. C. 2005, Icarus, 178, 517

Murray, C. D., & Dermott, S. F. 1999, Solar System Dynamics (Cambridge: Cambridge Univ. Press), (MD99)

Nelson, R. P. 2005, A&A, 443, 1067

Papaloizou, J.C.B., & Terquem, C. 2006, Rep. Prog. Phys., 69, 119

Peale, S. J. 1976, ARA&A, 14, 215

Press, W. H., Teukolsky, S. A., Vetterling, W. T., & Flannery, B. P. 1992, Numerical Rescipes in FORTRAN: The art of scientific computing (Cambridge: Cambridge Univ. Press)

Quillen, A. C. 2006, MNRAS, 365, 1367

Rivera, E. J., et al. 2005, ApJ, 634, 625

Tinney, C. G., Butler, R. P., Marcy, G. W., Jones, H. R. A., Laughlin, G., Carter, B. D., Bailey, J. A., & O'Toole, S. 2006, ApJ, 647, 594

Vogt, S. S., Butler, R. P., Marcy, G. W., Fischer, D. A., Henry, G. W., Laughlin, G., Wright, J. T., & Johnson, J. A. 2005, ApJ, 632, 638